Energy transfer characteristics of silicate glass doped with Er3+, Tm3+, and Ho3+ for 2 m emission

Ming Li, Xueqiang Liu, Yanyan Guo, Lili Hu, and Junjie Zhang

Citation: Journal of Applied Physics **114**, 243501 (2013); doi: 10.1063/1.4852535
View online: http://dx.doi.org/10.1063/1.4852535
View Table of Contents: http://scitation.aip.org/content/aip/journal/jap/114/24?ver=pdfcov
Published by the AIP Publishing

Energy transfer characteristics of silicate glass doped with Er^{3+}, Tm^{3+}, and Ho^{3+} for $\sim 2\,\mu m$ emission

Ming Li,[1,2] Xueqiang Liu,[1,2] Yanyan Guo,[3] Lili Hu,[1] and Junjie Zhang[4,a)]
[1]*Key Laboratory of Materials for High Power Laser, Shanghai Institute of Optics and Fine Mechanics, Chinese Academy of Sciences, Shanghai 201800, People's Republic of China*
[2]*Graduate School of Chinese Academy of Sciences, Beijing 100039, People's Republic of China*
[3]*College of Materials Science and Engineering, Changchun University of Science and Technology, Changchun 130022, People's Republic of China*
[4]*College of Materials Science and Engineering, China Jiliang University, Hangzhou 310 018, People's Republic of China*

(Received 2 July 2013; accepted 6 December 2013; published online 23 December 2013)

A $Er^{3+}/Tm^{3+}/Ho^{3+}$ tri-doped silicate glass with good thermal stability is prepared by melt-quenching method. Efficient $\sim 2\,\mu m$ emission is observed under 808 nm laser excitation. It is found that the $2.0\,\mu m$ emission of Ho^{3+} can be enhanced under the excitation at 808 nm by incorporating Er^{3+} and Tm^{3+}. Based on the measurement of absorption spectra, the Judd–Ofelt intensity parameters, radiation emission probability, and branching ratio are calculated to evaluate the spectroscopic properties simultaneously. The maximum value of emission cross section of Ho^{3+} is 3.54×10^{-21} cm^2 at 2008 nm. Additionally, the phonon assistance and the micro-parameters in the energy transfer process are quantitatively analyzed by using Dexter model. The energy transfer coefficient from Tm^{3+} to Ho^{3+} can reach as high as 21.44×10^{-40} cm^6/s, respectively. The emission property together with good thermal property indicates that $Er^{3+}/Tm^{3+}/Ho^{3+}$ tri-doped silicate glass is a potential kind of laser glass for efficient $2\,\mu m$ laser. © *2013 AIP Publishing LLC*.
[http://dx.doi.org/10.1063/1.4852535]

I. INTRODUCTION

Mid-infrared fiber lasers around $2\,\mu m$ have been attracting more and more attention in various useful applications including biomedical, remote sensing, light detection and ranging (LIDAR), and military.[1–4] It is well known that the laser around $2\,\mu m$ can be obtained from the Tm^{3+}:$^3F_4 \rightarrow {}^3H_6$ transition and Ho^{3+}:$^5I_7 \rightarrow {}^5I_8$ transition. Compared with Tm^{3+}, the broad emission band is broader and the emission cross section is much higher.[5,6] Moreover, the longer fluorescence lifetime of Ho^{3+} is in favor of Q-switched laser.[6,7] Therefore, ever since the first laser action at around $2\,\mu m$ from Ho^{3+} doped $CaWO_4$ crystal is reported in 1962, a considerable amount of work has been focused on $2\,\mu m$ laser emission from Ho^{3+} doped crystals and glasses.[8] However, despite a considerable amount of work on $2\,\mu m$ emission from Ho^{3+} singly doped glasses, the laser characteristics of the $2\,\mu m$ are not satisfactory since there are no readily available commercial laser diodes for pumping Ho^{3+} ions, leading to limited efficient laser operation. Besides, the non-radiative transition is a dominant process which can significantly reduce laser efficiency in Ho^{3+} singly doped silica fiber.[9,10] To enhance pump absorption, Ho^{3+} doped glasses have been sensitized with Er^{3+}, Tm^{3+}, or Yb^{3+} ions. It has been demonstrated that glasses co-doped or tri-doped with certain rare-earth ions may result in increased intensity of the desired emission in a number of cases and the energy transfer mechanisms between sensitizer ions and Ho^{3+} ions have also been investigated in Tm^{3+}/Ho^{3+}, Yb^{3+}/Ho^{3+}, and $Yb^{3+}/Tm^{3+}/Ho^{3+}$ glass.[11–13] Nevertheless, there are few reports about the $2.0\,\mu m$ emission in $Er^{3+}/Tm^{3+}/Ho^{3+}$ tri-doped glass system.[14,15]

In order to get powerful infrared emissions from Ho^{3+}, the host glass is another factor to be considered as important as the sensitizer. Although, CW high power (83 W) cladding-pumped Tm^{3+}/Ho^{3+} co-doped silica fiber laser has already been demonstrated with high slope efficiency (42%), it still suffers many problems for practical fiber laser applications.[4] For instance, in the operation of Q-switching, active mode-locking and passive mode-locking, almost all of the reported Ho-based pulsed lasers are bulky crystal lasers, so the maximum Ho^{3+} doping concentration is limited.

In the present work, silicate glass is chosen as the host material. Silicate glass means multi-component glass with SiO_2 as glass network former. In contrast to silica glass, silicate glasses contain glass network modifiers such as alkali ions and alkaline metal ions and the content of SiO_2 is not higher than 80 mol. % in most cases. Due to its less defined glass networking broken by the glass network modifiers, silicate glasses are capable of dissolving a much higher concentration of rare-earth ions.[16] Higher rare-earth oxide solubility helps in enabling efficient cross-relaxation energy transfer, greatly improving the quantum efficiency and reducing the device length in silicate fibers.[17,18] Recently single-frequency laser operation and passively mode-locked fiber laser in silicate fiber lasers have been demonstrated.[19,20] Meanwhile, the main glass network former of our silicate glass host is SiO_2, the same material as standard silica glass fiber. Relatively

a)Author to whom correspondence should be addressed: Electronic mail: jjzhang@mail.siom.ac.cn. Tel.: +86 571 87676298. Present address: College of Materials Science and Engineering, China Jiliang University, Hangzhou 310 018, People's Republic of China.

low thermal expansion coefficient, good physical and chemical properties, higher thermal stock resistance, and better compatibility with silica fiber make silicate glass more suitable compared to other multi-component glasses such as fluoride glasses, tellurite glasses, and germanate glasses.

The present work is devoted to the analysis of the infrared emission characteristics and energy transfer mechanism in $Er^{3+}/Tm^{3+}/Ho^{3+}$ tri-doped silicate glasses. Judd-Ofelt intensity parameters have been determined to evaluate the radiative properties. Besides, the relative energy transfer mechanisms and micro-parameters of the energy transfer processes are systemically investigated.

II. EXPERIMENTAL

A. Material synthesis

The investigated silicate glasses have the following molar composition: $(58.5\text{-}x)SiO_2\text{-}2Al_2O_3\text{-}13CaO\text{-}25(Li_2O + Na_2O + K_2O)\text{-}0.5Ho_2O_3\text{-}1Tm_2O_3\text{-}xEr_2O_3$ (x = 0.5, 1, and 2 mol. %), which is hereafter donated as SHET-x. The molar concentrations of Tm_2O_3 and Ho_2O_3 are fixed as 1 mol. % and 0.5 mol. % according to the previous reports.[21] In addition, 0.5 mol. % Ho_2O_3 singly doped, 0.5 mol. % Ho_2O_3/1 mol. % Er_2O_3 doubly doped, and 0.5 mol. % Ho_2O_3/1 mol. % Tm_2O_3 doubly doped silicate glass are prepared for the comparison of absorption and emission denoted as SH, SHE, and SHT. The high purity rare-earth oxides Ho_2O_3, Tm_2O_3, and Er_2O_3 are doped into silicate glasses with varying amounts. Fifty-gram batches of the samples are weighed and mixed. The samples of silicate glass are melted in a platinum crucible at 1450 °C for 1 h. Then, the melts are poured into preheated molds and annealed for 4 h near the glass transition temperature before they are cooled to room temperature. Finally, the annealed samples are fabricated and polished to the size of 10 mm × 10 mm × 1 mm for the optical and spectroscopic measurements, while others are cut and polished for refractive index.

B. Measurements

The refractive index is measured on the prism minimum deviation method. The density is measured by the Archimedes method using distilled water as immersion liquid. The characteristic temperatures (temperature of glass transition Tg, temperature of onset crystallization peak Tx, and temperature of top crystallization peak Tp) of powder samples crushed down from the samples are determined by a NetzschSTA449/C differential scanning calorimeter (DSC) at a heating rate of 10 K/min with accuracy of ±1 °C by using a NETZSCH STA 409PC/PG. Furthermore, the absorption spectra are recorded with a Perkin-Elmer Lambda 900 UV/VIS/NIR spectrophotometer in the range of 370–2100 nm, and the emission spectra are measured with a Triax 320 type spectrometer (Jobin-Yvon Co., France) upon excitation at 808 nm. All the measurements are carried out at room temperature.

III. RESULTS AND DISCUSSION

A. Absorption spectrum and Judd-Ofelt analysis

Fig. 1 shows the absorption spectrum of SH, SHE, SHT, and SHET1 glass samples at room temperature in the wavelength region of 370–2100 nm. Due to the intrinsic bandgap absorption of the host glass, the absorption bands at a wavelength shorter than 370 nm could not be distinguished. Each assignment corresponds to the excited level of Ho^{3+}, Tm^{3+}, and Er^{3+} shown in the figure. The absorption bands corresponding to the transitions starting from the $^5I_8$ ground state to the higher levels $^5I_7$, $^5I_6$, $^5F_5$, ($^5F_4$,$^5S_2$),$^5F_3$, ($^5G_6$,$^5F_1$), $^5G_5$ centered at the respective wavelength of 1934, 1140, 646, 536, 486, 446, and 420 nm, are labeled. In absorption spectrum of SH glass sample, no absorption bands around 800 nm and 980 nm can be observed, so the conventional pumping wavelength of 808 or 980 nm is not applicable to excite the Ho^{3+}-singly doped glass sample. Nevertheless, the emergence of the absorption band around 800 nm due to the Tm^{3+}:$^3H_6 \rightarrow {}^3H_4$ and Er^{3+}:$^4I_{15/2} \rightarrow {}^4I_{9/2}$ transitions and the absorption band around 980 nm due to the Er^{3+}:$^4I_{15/2} \rightarrow {}^4I_{11/2}$ transition in SHET-1 glass sample indicate Tm^{3+} and Er^{3+} can act as an efficient sensitizer to Ho^{3+} in $Er^{3+}/Tm^{3+}/Ho^{3+}$ tri-doped silicate glass system.

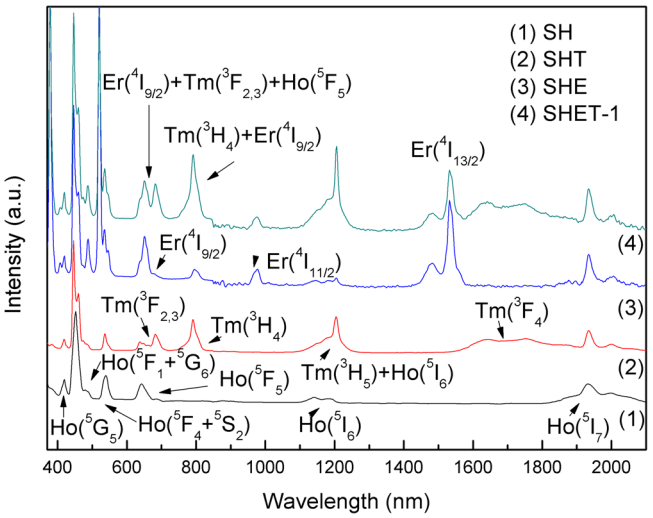

FIG. 1. Absorption spectrum of SH, SHE, SHT, and SHET-1 glass samples.

According to Judd-Ofelt theory,[22,23] the magnitude of the measured oscillator strengths and some important spectroscopic parameters of many trivalent rare earths doped glasses can be determined. Details of the theory and method have been well described earlier;[24,25] hence only results are presented here. The oscillator strength of the SH sample are shown in Table I, and the root-mean-square δ_{rms} between the experimental (f_{exp}) and calculated (f_{cal}) oscillator strengths deviation is calculated to be 0.76×10^{-6}, indicating that the calculation process is reliable. Additionally, the Judd-Ofelt intensity parameters ($\lambda = 2, 4, 6$) are important for the investigation of the local structure and bonding in the vicinity of rare earth ions. The Ω_λ values of Ho^{3+} are listed and compared with those obtained from other glasses in Table II. In the present glass system, the Ω_λ values follow the trend $\Omega_2 > \Omega_4 > \Omega_6$, which is similar to the most of silicate glass.[6,20] It can be observed that the Ω_2 of Ho^{3+} in our prepared silicate glass is larger than fluoride glass and fluorophosphate glass but smaller than tellurite glass and germanate glass. Previous studies revealed that the Ω_2

TABLE I. Measured and calculated oscillator strengths of SH glass.

Absorption	Wavelength (nm)	Oscillator strength (10^{-6})	
		f_{exp}	f_{cal}
$^5I_8 \rightarrow {}^5I_6$	1140	0.455	0.545
$^5I_8 \rightarrow {}^5F_5$	646	1.81	1.784
$^5I_8 \rightarrow {}^5F_4 + {}^5S_2$	536	2.577	1.733
$^5I_8 \rightarrow {}^5F_1 + {}^5G_6$	446	14.358	14.456
$^5I_8 \rightarrow {}^5G_5$	420	1.393	2.119

parameter is an environment sensitive parameter, and larger Ω_2 values represent a higher covalency of the chemical bond between rare earth and oxygen ions and lower symmetry.[26] By analyzing the value of Ω_2, it is revealed that covalency of the rare earth oxygen (Ho-O) bond in silicate glass is weaker than tellurite glass and germanate glass. Theoretically, O^{2-} ion possesses higher polarizability than F^- ion, so we can reasonably deduce that the asymmetry and covalent environment of Ho-O bond in silicate glass sample is stronger than that of fluorophosphate and ZBLAN glasses.[27] Besides, the Ω_6 parameter is vibronic dependent parameter, related to the rigidity and the viscosity of the host glass and the Ω_4/Ω_6 determines the spectroscopy quality of the materials.[26,28] The relatively low Ω_6 value indicates the higher rigidity of silicate host matrices. Moreover, the larger spectroscopic quality factor Ω_4/Ω_6 among the glasses listed in Table II indicates that silicate is a good matrix for 2 μm emission.

Some important radiative properties can be calculated by use of values of Ω_λ. Details of the theory and method have been well described earlier.[14,31] Table III shows the calculated predicted spontaneous transition probability (A_{rad}), total spontaneous transition probability ($\sum A_{rad}$), radiative lifetime (τ_{rad}), and branching ratios (β) of the optical transitions for the Ho^{3+}-doped silicate glass samples. The results show that the A_{rad} for Ho^{3+}:$^5I_7 \rightarrow {}^5I_8$ level is 63.52 s^{-1}, which is smaller than that of germanate glass (181.2 s^{-1}),[14] fluorophosphate glass (70.98 s^{-1}).[15] That is because the matrix elements $\|U^{(6)}\|$is much larger than $\|U^{(2)}\|$ and $\|U^{(4)}\|$ for the Ho^{3+}:$^5I_7 \rightarrow {}^5I_8$ transition and the A_{rad} is proportional to Ω_6 intensity parameter.[30] From Table II, it is noted that Ω_6 in the present glass is smaller than some other glasses. However, the value is higher than the value of 61.65 s^{-1} in another kind of Tm^{3+}/Ho^{3+} co-doped silicate glass.[29] Higher spontaneous emission probability provides a better opportunity to achieve 2 μm fluorescence from the Ho^{3+}: $^5I_7 \rightarrow {}^5I_8$ transition.

B. Fluorescence spectra

To investigate the infrared emission characteristics of the prepared $Er^{3+}/Tm^{3+}/Ho^{3+}$ tri-doped silicate glasses, fluorescence in the 1.3–2.2 μm region from SHT, SHE, SHET glass samples with varying dopant concentrations under excitation at 808 nm are measured at room temperature, and the resulting spectra are shown in Fig. 2. There are four emission bands centered at ~2 μm, 1.8 μm, 1.54 μm, and 1.47 μm, respectively. The emission at ~2.0 μm comes from the transition of Ho^{3+}:$^5I_7 \rightarrow {}^5I_8$ and the emission at 1.53 μm corresponds to the transition of the Er^{3+}:$^4I_{13/2} \rightarrow {}^4I_{15/2}$. Besides, the emission at 1.47 μm and 1.8 μm is originated from Tm^{3+}:$^3H_4 \rightarrow {}^3F_4$ transition and Tm^{3+}:$^3F_4 \rightarrow {}^3H_6$ transition, respectively.

As shown in Fig. 3, the intensity of emission bands at 1.47 μm, 1.54 μm, and 1.8 μm is extremely weak in our prepared SHET glass samples and the peak values at ~2.0 μm are listed in Fig. 4. Ho^{3+}/Tm^{3+} co-doping has been reported to be a suitable sensitizing method to achieve ~2.0 μm emission through pumping at 808 nm.[21] However, it can be found that the 1.8 μm Tm^{3+} fluorescence peak reduces obviously and the 1.47 μm Tm^{3+} fluorescence peak disappears, but the ~2.0 μm Ho^{3+} fluorescence peak increases in SHET glass samples after introducing Er^{3+} ions into SHT glass sample. Moreover, with the increase of Er^{3+} doping concentration, the emission intensity at ~2.0 μm increases smoothly with the increase of the Er^{3+} concentration up to 1 mol. % and the phenomenon of clustering and concentration quenching may appear when the concentration of Er_2O_3 increases to 2 mol. %. Besides, it is also worth noting that the 1.54 μm Er^{3+} fluorescence peak reduces intensely and the Ho^{3+} ~ 2.0 μm peak grows in SHET glass samples after introducing Tm^{3+} ions into SHE glass sample. It reveals the presence of an efficient energy transfer from Er^{3+} to Tm^{3+} ions and Tm^{3+} to Ho^{3+} ions, and the energy transfer mechanism is discussed later in Sec. III D. The peak intensity ratios of 2.0 μm to 1.54 μm and 1.8 μm are also presented in Fig. 5 and the values in tri-doped glass samples are much larger than those in co-doped ones. On the basis of fluorescence spectra, we suggest that both of Er^{3+} and Tm^{3+} are good sensitizers ion to enhance ~2.0 μm emission in Ho^{3+} doped silicate glass and $Er^{3+}/Tm^{3+}/Ho^{3+}$ tri-doping glass may be a more appropriate and significant sensitization way. The optimized doping concentration-ratio of Ho^{3+}, Tm^{3+}, and Er^{3+} for ~2.0 μm emission is 0.5:1:1 in our research.

C. Cross-sections and gain coefficient of Ho^{3+}

The absorption cross sections and emission cross sections are usually calculated in order to analyze the possible energy transfer between the doped rare earth ions.

TABLE II. J-O parameters Ω_λ of Ho^{3+} in various glasses.

Ω_λ (10^{-20} cm^2)	Fluoride	Fluorophosphate	Germanate	Tellurite	Phosphate	Silicate
Ω_2	1.86	2.08	10.5	5.3	3.33	3.57
Ω_4	1.90	3.11	3.35	3.4	3.01	1.86
Ω_6	1.32	1.50	3.28	1.2	0.61	0.84
Ω_4/Ω_6	1.44	2.07	1.02	2.83	4.93	2.21
Reference	29	15	14	30	29	This work

TABLE III. The predicted spontaneous transition probability (A), total spontaneous transition probability (ΣA), branching ratios (β), and radiative lifetimes (τ_{rad}) of silicate glass samples for various selected excited states of Ho^{3+}.

Transition	λ (nm)	$A_{rad}(s^{-1})$	ΣA_{rad} (s^{-1})	β(%)	τ_{rad} (ms)
Ho^{3+}: $^5I_7 \rightarrow {}^5I_8$	1934	63.52	63.52	100	15.74
Ho^{3+}: $^5I_6 \rightarrow {}^5I_8$	1140	91.11	116.16	78.44	8.61
Ho^{3+}: $^5I_6 \rightarrow {}^5I_7$	2777	25.04		21.56	
Ho^{3+}: $^5I_5 \rightarrow {}^5I_8$	887	32.46	84.01	38.64	11.90
Ho^{3+}: $^5I_5 \rightarrow {}^5I_7$	1638	42.33		50.39	
Ho^{3+}: $^5I_5 \rightarrow {}^5I_6$	3997	9.22		10.98	
Ho^{3+}: $^5I_4 \rightarrow {}^5I_8$	757	4.31	44.63	9.65	22.41
Ho^{3+}: $^5I_4 \rightarrow {}^5I_7$	1244	20.44		45.81	
Ho^{3+}: $^5I_4 \rightarrow {}^5I_6$	2253	15.40		34.52	
Ho^{3+}: $^5I_4 \rightarrow {}^5I_5$	5165	4.48		10.03	
Ho^{3+}: $^5F_5 \rightarrow {}^5I_8$	646	1099.02	1404.98	78.22	0.71
Ho^{3+}: $^5F_5 \rightarrow {}^5I_7$	970	268.40		19.10	
Ho^{3+}: $^5F_5 \rightarrow {}^5I_6$	1491	33.40		2.41	
Ho^{3+}: $^5F_5 \rightarrow {}^5I_5$	2378	3.71		0.26	
Ho^{3+}: $^5F_5 \rightarrow {}^5I_4$	4406	0.04		0.00	
Ho^{3+}: $^5S_2 \rightarrow {}^5I_8$	544	561.09	1077.22	52.09	0.93
Ho^{3+}: $^5S_2 \rightarrow {}^5I_7$	757	417.86		38.79	
Ho^{3+}: $^5S_2 \rightarrow {}^5I_6$	1041	75.15		6.98	
Ho^{3+}: $^5S_2 \rightarrow {}^5I_5$	1407	16.39		1.52	
Ho^{3+}: $^5S_2 \rightarrow {}^5I_4$	1933	6.37		0.59	
Ho^{3+}: $^5S_2 \rightarrow {}^5F_5$	3445	0.37		0.03	
Ho^{3+}: $^5F_4 \rightarrow {}^5I_8$	536	1944.20	2490.44	78.07	0.40
Ho^{3+}: $^5F_4 \rightarrow {}^5I_7$	742	274.17		11.01	
Ho^{3+}: $^5F_4 \rightarrow {}^5I_6$	1012	173.02		6.95	
Ho^{3+}: $^5F_4 \rightarrow {}^5I_5$	1355	73.78		2.96	
Ho^{3+}: $^5F_4 \rightarrow {}^5I_4$	1836	12.07		0.48	
Ho^{3+}: $^5F_4 \rightarrow {}^5F_5$	3148	13.20		0.52	
Ho^{3+}: $^5F_4 \rightarrow {}^5S_2$	36,448	0.00		0.00	

According to the measured absorption spectra shown in Fig. 1, the absorption cross-section (σ_{abs}) can be calculated by using Beer-Lambert equation

$$\sigma_{abs}(\lambda) = \frac{2.303\log\left[\frac{l_0(\lambda)}{l(\lambda)}\right]}{Nl}, \quad (1)$$

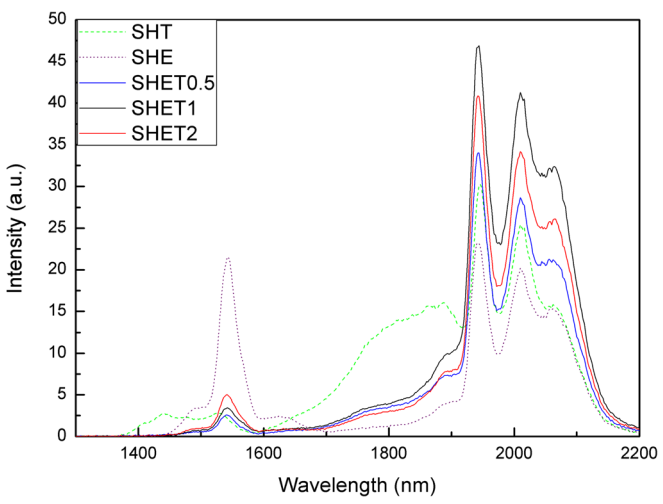

FIG. 2. Normalized fluorescence spectra of SHT, SHE, and SHET glass samples under the 808 nm excitation at room temperature.

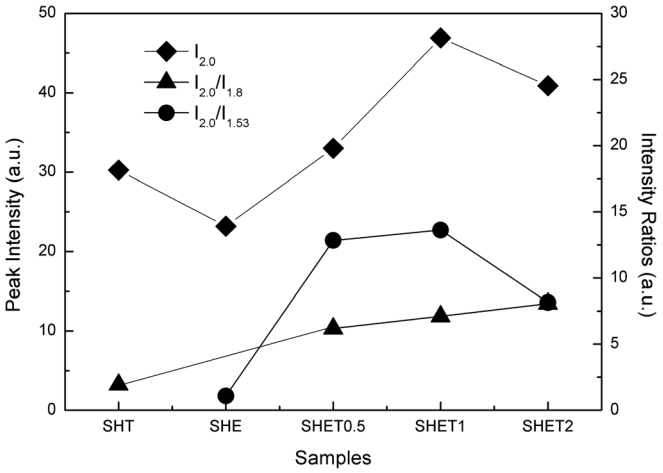

FIG. 3. Fluorescence peak intensity at ~2.0 μm (diamond) and the intensity ratios of $I_{2.0}/I_{1.8}$ (up-triangle) and $I_{2.0}/I_{1.54}$ (circle) in various samples.

where $l_0(\lambda)$ is the incident optical intensity, $l(\lambda)$ is the optical intensity throughout the sample, N is the rare earth ion density, and l is the sample thickness.

The emission cross section (σ_{em}) can be calculated from the absorption section by using the McCumber formula to evaluate the possibility of laser effect.[32]

$$\sigma_{em}(\lambda) = \sigma_{abs}(\lambda) \times \frac{Z_l}{Z_u} \times \exp\left(\frac{E_{zl} - hc\lambda^{-1}}{kT}\right), \quad (2)$$

where Z_u and Z_l are the partition functions of the upper and lower states, respectively, λ, k, and T are wavelength of the transition, Boltzmann's constant, and the temperature (here is the room temperature), and E_{ZL} is defined as the wavelength for the transition between the lower Stark sublevels of the emitting multiplets and the lower Stark sublevels of the receiving multiplets (zero-phonon line), respectively.

Fig. 4 shows the absorption (σ_{abs}) and emission (σ_{em}) cross sections of doped rare earth ions, and the corresponding transitions are indicated in the figure caption. Theoretically, larger absorption cross section means pump energy can be fully utilized. As shown in the figure, it can be found that the absorption cross section of Tm^{3+}:$^3H_6 \rightarrow {}^3H_4$ is much larger than that of Er^{3+}:$^4I_{9/2} \rightarrow {}^4I_{15/2}$ at ~800 nm and the maximum of σ_{abs} for Tm^{3+}:$^3H_6 \rightarrow {}^3H_4$ transition in the SHET-1 glass sample is calculated to be 3.3×10^{-21} cm^2 at 793 nm. Besides, it is generally desirable for the emission cross section to be as large as possible to provide a high gain. We can see that the calculated maximum σ_{em} for Ho^{3+}:$^5I_7 \rightarrow {}^5I_8$ transition in SHET glass sample is 3.54×10^{-21} cm^2 at 2008 nm. The σ_{em} is larger than that in Tm^{3+}/Ho^{3+} co-doped fluoride glass (2.47×10^{-21} cm^2)[33] and that in Tm^{3+}/Ho^{3+} co-doped silicate glass (3.54×10^{-21} cm^2),[21] but smaller than that in Yb^{3+}/Ho^{3+} co-doped tellurite glass (10.00×10^{-21} cm^2)[34] and that in $Er^{3+}/Tm^{3+}/Ho^{3+}$ tri-doped germanate glass (8.00×10^{-21} cm^2),[14] mainly due to the low refractive index and spontaneous transition probability.

On the basis of the σ_{abs} and σ_{em}, it is interesting to calculate the wavelength dependence of net gain as a function

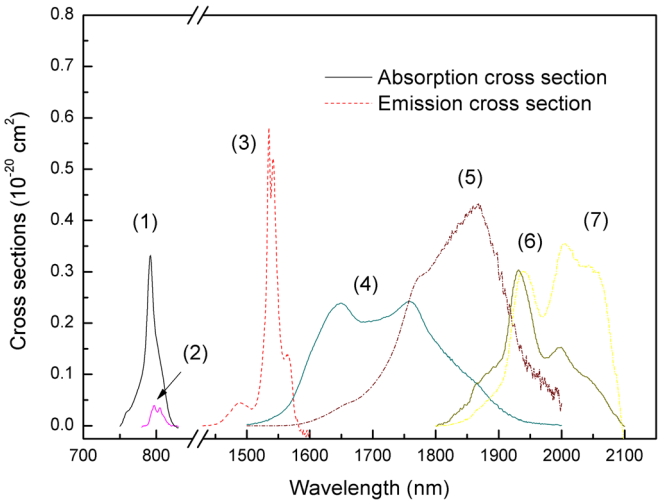

FIG. 4. Absorption cross sections and emission cross sections of rare earth ion doped samples. (1) Tm^{3+}:$^3H_6 \rightarrow {}^3H_4$; (2)$Er^{3+}$:$^4I_{15/2} \rightarrow {}^4I_{9/2}$; (3)$Er^{3+}$:$^4I_{13/2} \rightarrow {}^4I_{15/2}$; (4)$Tm^{3+}$:$^3H_6 \rightarrow {}^3F_4$; (5)$Tm^{3+}$:$^3F_4 \rightarrow {}^3H_6$; (6)$Ho^{3+}$:$^5I_8 \rightarrow {}^5I_7$; (7)$Ho^{3+}$:$^5I_7 \rightarrow {}^5I_8$.

of population inversion for the upper laser state in order to determine the gain property qualitatively. The gain cross-section spectrum $\sigma_g(\lambda)$, can be calculated by

$$\sigma_g(\lambda) = N[P\sigma_{em}(\lambda) - (1-P)\sigma_{abs}(\lambda)], \quad (3)$$

where P is the population inversion given by the ratio between the population of Ho^{3+}:$^5I_7$ level and the total Ho^{3+} concentration and N is the total concentration of Ho^{3+}. The calculated gain coefficient versus wavelength for different population inversion parameter P is shown in Fig. 5 and the positive gain is obtained when $P > 0.4$. It is noted that the gain coefficient increases and the gain band extends to longer wavelength with the increased value of P. This behavior is a typical characteristic of a quasi-three level system.[35]

D. Energy transfer mechanism

The energy-level diagram shown in Fig. 6 is helpful to understand the mechanism of energy transfer between Er^{3+}, Tm^{3+}, and Ho^{3+} pumped at 808 nm. And this mechanism can be specifically explained: First, both Er^{3+} and Tm^{3+} ions can be excited to Er^{3+}:$^4I_{9/2}$ and Tm^{3+}:$^3H_4$ state by ground state absorption (GSA) when sample is pumped by 808 nm LD. Then, the excited Er^{3+} ions in $^4I_{9/2}$ state decay to Er^{3+}:$^4I_{13/2}$ via double nonradiative relaxation by multi-phonon emission. After that, part of Er^{3+} ions in $^4I_{13/2}$ state relaxes to the ground state $^4I_{15/2}$ generating 1540 nm emission, and the other part decay nonradiatively to the ground state $^4I_{15/2}$ by exciting neighboring Tm^{3+} and Ho^{3+} ions. At the same time, a small amount of the Tm^{3+} in $^3H_4$ state decay radiatively, producing 1.47 μm emission, although this cannot be observed in our prepared tri-doped glass samples in the fluorescence spectra; furthermore, the cross-relaxation between Tm^{3+}:$^3H_4$ and $^3H_6$ state takes place and produces two Tm^{3+} ions at the $^3F_4$ state, which can enhance the pump quantum efficiency. Once the Tm^{3+}:$^3F_4$ state is populated, the transition $^3F_4 \rightarrow {}^3H_6$ generates1.8 μm emission, which we can observe in SHT glass sample clearly, and the energy of the Tm^{3+}:$^3F_4$ also transfers to Ho^{3+}:$^5I_7$ state, which is similar to the typical Tm^{3+}/Ho^{3+} co-doped glass system. Finally, 2 μm fluorescence will be emitted from the Ho^{3+}:$^5I_7 \rightarrow {}^5I_8$ transition.

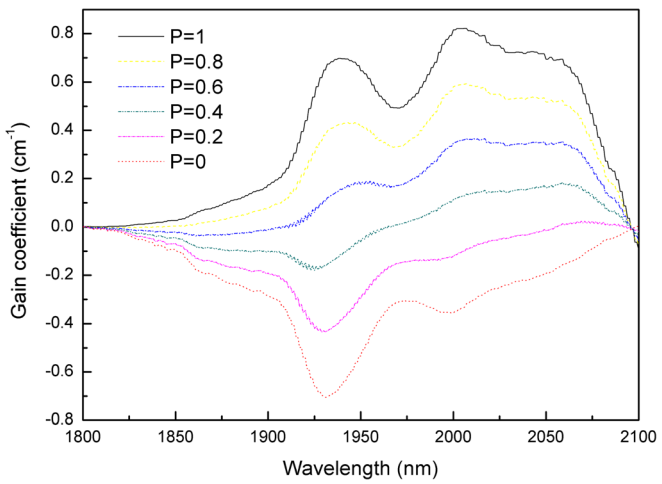

FIG. 5. Gain coefficient corresponding to Ho^{3+}:$^5I_7 \rightarrow {}^5I_8$ transition.

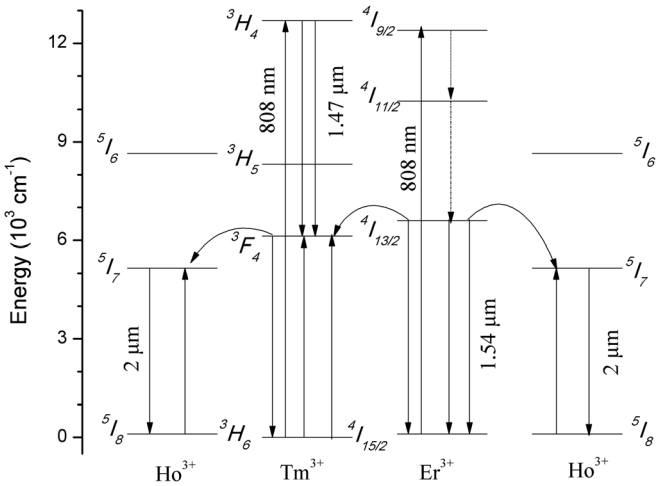

FIG. 6. Energy-level diagram and energy transfer ketch-map between Er^{3+}, Tm^{3+}, and Ho^{3+} when pumped at 808 nm.

As shown in Fig. 2, the 1.54 μm,1.8 μm, and 2.0 μm emissions due to Er^{3+}:$^4I_{13/2} \rightarrow {}^4I_{15/2}$, Tm^{3+}:$^3F_4 \rightarrow {}^3H_6$, and Ho^{3+}:$^5I_7 \rightarrow {}^5I_8$ transition differ greatly in intensity among SHE, SHT, and SHET, which is due to the energy transfer among Er^{3+}, Tm^{3+}, and Ho^{3+} ions. When the Er^{3+}:$^4I_{13/2}$ state is saturated, most of the energy transfer to neighboring Tm^{3+}:$^3F_4$ state and 1.54 μm Er^{3+} fluorescence peak reduces intensely in SHET glass samples after introducing Tm^{3+} ions into SHE glass sample. At the same time, the $Ho^{3+} \sim 2.0$ μm peak grows in SHET glass samples, which can be attributed to the energy transfer from Tm^{3+}:$^3F_4$ state to Ho^{3+}:$^5I_7$ state. We have demonstrated that co-doping of Tm^{3+} as a sensitizer to Ho^{3+} is beneficial to 2.0 μm emission in silicate glass.[21] The results indicate that $Er^{3+}/Tm^{3+}/Ho^{3+}$ tri-doping glasses are suitable sensitizing methods to achieve strong 2.0 μm emission through pumping at 808 nm.

In order to prove the sensitization and optimize the corresponding laser system, the microscopic probability rate of energy transfer between rare earth ions is required. Fortunately, a method for estimating the microscopic probability rate of energy transfer between rare-earth ions in solids has been developed by Förster and Dexter.[36]

According to the Dexter's model, the extent of energy transfer depends on the spectral overlap of donor's emission and acceptor's absorption. In the case of resonant energy transfer between donors and accepters, the model predicts a linear relationship between the transfer probability (P_{ET}) and the spectral overlap between donor emission and acceptor absorption bands[28]

$$P_{ET} \propto \int \frac{f_D(E) f_A(E)}{E^2} dE \tag{4}$$

where $f_D(E)$ and $f_A(E)$ are the line-shape functions of the acceptor absorption and donor emission cross sections, respectively. In Fig. 3, it should be noted that there is some overlap between σ_{abs} of Tm^{3+}:$^3F_4 \rightarrow {}^3H_6$ transition and σ_{em} of Er^{3+}:$^4I_{13/2} \rightarrow {}^4I_{15/2}$ transition, σ_{abs} of Ho^{3+}:$^5I_7 \rightarrow {}^5I_8$ transition, and σ_{em} of Tm^{3+}:$^3F_4 \rightarrow {}^3H_6$ transition, which indicates the possibility of direct energy transfer between corresponding rare earth ions in present glass.

If the phonon participated process considered, the transfer constant for direct transfer (D-A) can be obtained using the following equation:

$$C_{D-A} = \frac{3cg_{low}^{D}}{8\pi^4 n^2 g_{up}^{D}} \sum_{m=0}^{\infty} e^{-(2\bar{n}+1)S_0} \frac{S_0^m}{m!} (\bar{n}+1)^m \int \sigma_{ems}^{D}(\lambda_m^+) \sigma_{abs}^{A}(\lambda) d\lambda, \tag{5}$$

where c is the light speed, n is the refractive index, g_{low}^D/g_{up}^D is the degeneracy of the respective lower and upper levels of the donor, $\hbar\omega_0$ is the max phonon energy, $\bar{n} = 1/(e^{\hbar\omega_0/kT} - 1)$ is the average occupancy of phonon mode at temperature T, m is number of the phonons that participate in the energy transfer, and S_0 is Huang-Rhys factor, $\lambda_m^+ = 1/(1/\lambda - m\hbar\omega_0)$ is the wavelength with m phonon creation.

Using the Eq. (5), SHET1 shows the most intense emission at ~2.0 μm among the samples, the energy transfer properties among Er^{3+}, Tm^{3+}, and Ho^{3+} ions in this sample are calculated and listed in Table IV. The result shows that the direct transfer of Tm^{3+}:$^3F_4 \rightarrow Ho^{3+}$:$^5I_7$ is found to be a quasiresonant process with nonphonon 61.81%, having a participation of 1 (29.82%) and 2 (0.07%) phonons. The direct transfer of Er^{3+}:$^4I_{13/2} \rightarrow Tm^{3+}$:$^3F_4$ is found to be a quasiresonant process with nonphonon 24.98%, having a participation of 1 (75.02%) phonon emission, while the direct transfer of Er^{3+}:$^4I_{13/2} \rightarrow Ho^{3+}$:$^5I_7$ needs the assistance of 1 (99.85%) phonon emission. As is known, probability of nonresonant phonon-assisted energy transfer involving phonon generation is always lower than the resonant process. It demonstrates that the resonant transfer Tm^{3+}:$^3F_4 \rightarrow Ho^{3+}$:$^5I_7$ is the most probable microscopic process to occur in contrast with the nonresonant Er^{3+}:$^4I_{13/2} \rightarrow Ho^{3+}$:$^5I_7$ in the silicate glass.

TABLE IV. Calculated microscopic parameters for energy transfer process in SHET-1 glass sample, and the number of phonons necessary to assist the energy transfer as well as the percentage of each phonon participation in the process, are indicated.

Energy Transfer	N (number of phonons) (% phonon assisted)			C_{D-A} (10^{-40} cm^6 s)	C_{D-D} (10^{-40} cm^6 s)
$Tm^{3+} \rightarrow Ho^{3+}$	0	1	2	21.44	…
	61.81	29.82	0.07		
$Er^{3+} \rightarrow Tm^{3+}$	0		1	4.58	…
	24.98		75.02		
$Er^{3+} \rightarrow Ho^{3+}$	1		2	0.49	…
	99.85		0.15		
$Tm^{3+} \rightarrow Tm^{3+}$	0		1	…	36.64
	92.56		7.44		
$Er^{3+} \rightarrow Er^{3+}$	0		1	…	85.07
	99.83		0.017		

For the nonresonant energy transfer, the Dexter model can be generalized to the nonresonant phonon assisted energy transfer case taking account of phonon energy involved (E_{PH}) as well as the phonon density. Thus, the transfer probability can be estimated from the phonon modified spectral overlap integral I(E_{PH}). If we assume that only one phonon is involved, P(ET) can be expressed as

$$P(ET) \propto I(E_{PH}) = \frac{e^{E_{PH}/k_BT}}{e^{E_{PH}/k_BT} - 1} \int \frac{f_D(E - E_{PH}) f_A(E)}{E^2} dE, \tag{6}$$

where k_B and T are Boltzmann constant and absolute temperature, respectively. Based on the absorption and emission spectra in Fig. 4, the energy transfer probability has been calculated as a function of phonon energy in the range of 0–2200 cm^{-1}, and presented in Fig. 7. It can be seen that the phonon assisted overlap integral increases with an increase in phonon energy and it reaches a maximum for phonons with energy of about 800 cm^{-1} for Er^{3+}:$^4I_{13/2} \rightarrow Tm^{3+}$:$^3F_4$ transition and 1340 cm^{-1} for Er^{3+}:$^4I_{13/2} \rightarrow Ho^{3+}$:$^5I_7$ transition. For further increase in the phonon energy, the energy transfer probability decreases and diminishes. As phonon

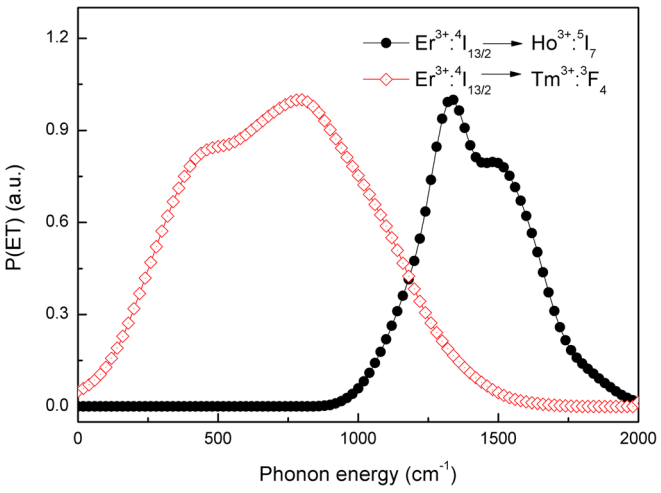

FIG. 7. Energy transfer probability (vs) phonon energy in SHET glass sample.

TABLE V. Comparison of DSC parameters in various glasses.

Glass compositions	Tg (°C)	Tx (°C)	ΔT = Tx-Tg (°C)	k_{gl}	References
Fluoride glass	267	345	78	0.162	41
Fluorophosphate glass	435	564	129	0.250	13
Tellurite glass	348	495	147	0.266	42
Germanate glass	611	840	229	0.290	14
Phosphate glass	410	500	90	0.095	43
Silicate glass	563	896	333	0.375	This work

energy of present silicate glass is $\sim 1050\,cm^{-1}$, about one or less phonon is required to bridge the energy gap between Er^{3+}:$^4I_{13/2}$ and Tm^{3+}:$^5I_7$ state, while one or more phonons are required to bridge the energy gap between Er^{3+}:$^4I_{13/2}$ and Tm^{3+}:$^3F_4$ state. Assisted with the host phonon, the energy level mismatch can be covered. In this way, it can be expected to achieve 2.0 μm emission with high energy transfer efficiency from donors to acceptors in $Er^{3+}/Tm^{3+}/Ho^{3+}$ tri-doped silicate glass.

E. Thermal stability

As a part of structural investigation on the silicate glass, thermal relaxation properties are measured using a DSC. The values of Tg, Tx, and Tp are 563, 896, and 968 °C in host glass sample. Dietzel introduced the glass criterion, $\Delta T = T_x - T_g$, which is often used for evaluating the glass forming ability and the larger super cooled liquid region ΔT parameter means the better thermal stability against crystallization.[37,38] Usually, ΔT should be more than 120 °C to minimize probability of crystallization during the drawing process.[39] Hruby developed the H_r criterion, $H_r = (T_x - T_g)/(T_m - T_p)$. T_m is the melting temperature of glass.[40] The glass formation factor of the materials is given by parameter $k_{gl} = (T_x - T_g)/(T_m - T_g)$ and is more suitable for estimating the glass thermal stability than ΔT. The larger the k_{gl}, the better the glass forming ability. The glass forming ability can be estimated by using these characteristic temperatures. The existing ability criterion parameters k_{gl} is 0.375, respectively. Compared with other glass matrices in Table V, the silicate glass samples in this study prove a better thermal stability, which are greatly beneficial to optical fiber drawing.

IV. CONCLUSION

In summary, we have prepared samples of $Er^{3+}/Tm^{3+}/Ho^{3+}$ tri-doped silicate glass by the melt-quenching method. The 2 μm emission characteristics of Ho^{3+} with Er^{3+} and Tm^{3+} sensitization upon 808 nm excitation have been reported. The Judd–Ofelt theory and McCumber formula have been used to calculate the intensity parameters and emission cross sections. For the present glass, the predicted spontaneous transition probability and emission cross-section of Ho^{3+}:$^5I_7 \rightarrow {}^5I_8$ transition reaches $63.52\,s^{-1}$ and $3.54 \times 10^{-21}\,cm^2$ at the wavelength of 2008 nm, respectively. It is found Er^{3+} and Tm^{3+} ions can transfer their energy to Ho^{3+} with high efficiency, which can enhance the pump absorption. Dexter's model has been used to analyze the energy transfer process and energy transfer coefficient from Tm^{3+} to Ho^{3+} can reach as high as $21.44 \times 10^{-40}\,cm^6/s$. Dexter's model and multiphoton relaxation theory have been used to analyze the energy transfer process between Er^{3+} and Tm^{3+}/Ho^{3+} ions. The present results indicate that this $Er^{3+}/Tm^{3+}/Ho^{3+}$ triply doped silicate glass with good thermal stability can be selected as a kind of potential medium material for ~2 μm laser.

ACKNOWLEDGMENTS

This work was financially supported by National Natural Science Foundation of China (No. 51172252).

[1]C. Guo, D. Shen, J. Long, and F. Wang, Chin. Opt. Lett. **10**, 091406 (2012).
[2]J. Yang, Y. Tang, and J. Xu, Photon. Res. **1**, 52 (2013).
[3]G. Li, Y. Gu, B. Yao, L. Shan, and Y. Wang, Chin. Opt. Lett. **11**, 091404 (2013).
[4]S. D. Jackson, A. Sabella, A. Hemming, S. Bennetts, and D. G. Lancaster, Opt. Lett. **32**, 241 (2007).
[5]S. D. Jackson, F. Bugge, and G. Erbert, Opt. Lett. **32**, 2496 (2007).
[6]S. D. Jackson, Laser Photon. Rev. **3**, 466 (2009).
[7]R. Xu, J. Pan, L. Hu, and J. Zhang, J. Appl. Phys. **108**, 043522 (2010).
[8]L. J. Johson, G. D. Boyd, and K. Nassau, Proc IRE **50**, 87 (1962).
[9]H. W. Gandy and R. J. Ginther, Proc IRE **50**, 2113 (1962).
[10]D. C. Hanna, R. M. Percival, and R. G. Smart, Electron Lett. **25**, 593 (1989).
[11]G. Gao, L. Hu, H. Fan, G. Wang, K. Li, S. Feng, S. Fan, H. Chen, J. Pan, and J. Zhang, Opt. Mater. **32**, 402 (2009).
[12]G. Bai, Y. Guo, L. Hu, and J. Zhang, Opt. Mater. **33**, 1316 (2011).
[13]M. Wang, L. Yi, G. Wang, L. Hu, and J. Zhang, Chin. Opt. Lett. **7**, 1035 (2009).
[14]R. Xu, M. Wang, Y. Tian, L. Hu, and J. Zhang, J. Appl. Phys. **109**, 053503 (2011).
[15]M. Wang, L. Yi, G. Wang, L. Hu, and J. Zhang, Solid State Commun. **149**, 1216 (2009).
[16]S. Jiang, "Thulium-doped heavy metal oxide glasses for 2 μm lasers," U.S. patent 7,298,768 (2007).
[17]M. Li, G. Bai, Y. Guo, L. Hu, and J. Zhang, J. Lumin. **132**, 1830 (2012).
[18]X. Wang, L. Hu, K. Li, Y. Tian, and S. Fan, Chin. Opt. Lett. **10**, 101601 (2012).
[19]Q. Wang, J. Geng, T. Luo, and S. Jiang, Opt. Lett. **34**, 3616 (2009).
[20]J. Geng, Q. Wang, T. Luo, and S. Jiang, Opt. Lett. **34**, 3493 (2009).
[21]M. Li, Y. Guo, G. Bai, Y. Tian, L. Hu, and J. Zhang, J. Quantum Spectrosc. Radiat. Transfer **127**, 70 (2013).
[22]B. R. Judd, Phys. Rev. **127**, 750 (1962).
[23]G. S. Ofelt, J. Chem. Phys. **37**, 511 (1962).
[24]M. Shojiya, Y. Kawamoto, and K. Kadono, J. Appl. Phys. **89**, 4944 (2001).
[25]J. Ding, Y. Chen, W. Chen, L. Hu, and G. Boulon, Chin. Opt. Lett. **10**, 071602 (2012).
[26]C. K. Jorgensen and R. Reisfeld, J. Less Common Met. **93**, 107 (1983).
[27]R. D. Shannon, J. Appl. Phys. **73**, 348 (1993).
[28]G. Zhao, Y. Tian, H. Fan, J. Zhang, and L. Hu, Chin. Opt. Lett. **10**, 091601 (2012).
[29]B. Peng and T. Izumitani, Opt. Mater. **4**, 797 (1995).
[30]G. Chen, Q. Zhang, G. Yang, and Z. Jiang, J. Fluoresc. **17**, 301 (2007).
[31]S. Guan, Y. Tian, Y. Guo, L. Hu, and J. Zhang, Chin. Opt. Lett. **10**, 071603 (2012).
[32]D. E. McCumber, Phys. Rev. **134**, A299 (1964).
[33]A. Florez, S. L. Oliveira, M. Florez, L. A. Gomeza, and L. A. O. Nunes, J. Alloys Compd. **418**, 238 (2006).
[34]K. Li, Q. Zhang, S. Fan, L. Zhang, J. Zhang, and L. Hu, Opt. Mater. **33**, 31 (2010).
[35]X. L. Zou and H. Toratani, J. Non-Cryst. Solids **195**, 113 (1996).
[36]D. L. Dexter, J. Chem. Phys. **21**, 836 (1953).
[37]A. Dietzel, Glastech. Ber. **22**, 41 (1968).

[38]N. H. Chan, R. K. Sharma, and D. M. Smyth, J. Am. Ceram. Soc. **65**, 167 (1982).
[39]Z. Y. Yang, T. Luo, S. B. Jiang, J. H. Geng, and P. Lucas, Opt. Lett. **35**, 3360 (2010).
[40]A. Hruby, Czech. J. Phys. B **22**, 1187 (1972).
[41]M. Wang, L. Yi, Y. Chen, C. Yu, G. Wang, L. Hu, and J. Zhang, Mater. Chem. Phys. **114**, 295 (2009).
[42]G. Gao, G. Wang, C. Yu, J. Zhang, and L. Hu, J. Lumin. **129**, 1042 (2009).
[43]A. Kermaoui and F. Pellé, J. Alloys Compd. **469**, 601 (2009).